

Subspace Clustering using Ensembles of K -Subspaces

John Lipor, David Hong, Dejiao Zhang, and Laura Balzano
 Department of Electrical and Computer Engineering
 University of Michigan, Ann Arbor
 {lipor,dahong,dejiao,girasole}@umich.edu

Abstract

We present a novel approach to the subspace clustering problem that leverages ensembles of the K -subspaces (KSS) algorithm via the evidence accumulation clustering framework. Our algorithm forms a co-association matrix whose (i, j) th entry is the number of times points i and j are clustered together by several runs of KSS with random initializations. We analyze the entries of this co-association matrix and show that a naïve version of our algorithm can recover subspaces for points drawn from the same conditions as the Thresholded Subspace Clustering algorithm. We show on synthetic data that our method performs well under subspaces with large intersection, subspaces with small principal angles, and noisy data. Finally, we provide a variant of our algorithm that achieves state-of-the-art performance across several benchmark datasets, including a resulting error for the COIL-20 database that is less than half that achieved by existing algorithms.

I. INTRODUCTION

In modern computer vision problems such as facial recognition [1] and object tracking [2], researchers have found success applying the union of subspaces (UoS) model, in which data vectors lie near one of several subspaces. Under this model, the goal is to simultaneously identify these underlying subspaces and cluster the points according to their nearest subspace. Algorithms designed to solve this problem fall under the category of *subspace clustering*, a topic that has received a great deal of attention in recent years [3] due to its efficacy on real-world datasets such as the Extended Yale Face Database B [4] and the MNIST handwritten digit database [5].

One of the earliest approaches to solving the subspace clustering problem involves an iterative method in the spirit of K -means, known as K -subspaces (KSS) [6], [7], [8], which alternates between assigning points to clusters and estimating the subspace basis associated with each cluster. As this algorithm is only guaranteed to converge to a local minimum, in practice one runs many instances of the algorithm and chooses the final clustering as the one that produces the minimum cost. Although its empirical performance is limited, KSS continues to serve as a benchmark for subspace clustering algorithms, in part due to its computational efficiency and simplicity. Therefore, a deeper understanding of this method is an important contribution in the area of subspace clustering and a contribution of this paper.

While the KSS cost function and alternating algorithm are perhaps the most natural approach for the subspace clustering problem, it is known that there is a set of initializations of nonzero measure from which the algorithm will converge to a point other than the global minimizer.¹ Our key observation is that even those “bad” initializations very commonly give some partially-correct clustering behavior and may be combined to form a more accurate clustering algorithm.

Our contributions are as follows. We introduce a novel application of the well-known *evidence accumulation clustering* framework [9] that leverages ensembles of the KSS algorithm to perform subspace clustering. By combining the results of many random initializations of KSS, this algorithm obtains an affinity matrix (known as a *co-association matrix*), to which we apply spectral clustering. We provide theoretical guarantees regarding the resulting affinity matrix that lead to recovery guarantees for the subspace clustering problem. We show that our method is extremely effective on both synthetic and real datasets; we show on synthetic data that our method has superior performance for subspaces that are extremely close together. Further, we show that a variant of our algorithm achieves state-of-the-art performance on several real datasets, including error on the COIL-20 image database and full Yale B database that are 24% and 54% better than state-of-the-art, respectively. Finally, since our method relies on multiple independent initializations, it is inherently parallelizable. To the best of our knowledge, we provide the first theoretical guarantees characterizing the co-association matrix resulting from evidence accumulation, as well as the first recovery guarantees for any variant of the KSS algorithm.

II. PROBLEM FORMULATION & RELATED WORK

Consider a collection of points $\mathcal{X} = \{x_1, \dots, x_N\}$ in \mathbb{R}^D belonging to a union of K subspaces $\mathcal{S}_1, \dots, \mathcal{S}_K$ having dimensions d_1, \dots, d_K . Let $X \in \mathbb{R}^{D \times N}$ denote the matrix whose columns are the elements of \mathcal{X} . The goal of subspace clustering is to label points in the unknown union of K subspaces according to their nearest subspace. Once the clusters have been obtained, the corresponding subspace bases can be recovered using principal components analysis (PCA).

¹We prove this fact for the simple case of two one-dimensional subspaces in \mathbb{R}^2 in Appendix B.

Most state-of-the-art approaches to subspace clustering rely on a *self-expressiveness* property of the data, which informally states that points in the UoS model can be most efficiently represented by other points within the same subspace. These methods typically use a self-expressive data cost function that is regularized to enforce efficient representation as follows:

$$\begin{aligned} \min_Z \quad & \|X - XZ\|_F^2 + \|Z\| \\ \text{subject to} \quad & \text{diag}(Z) = 0, \end{aligned}$$

where $\|Z\|$ may be the 1-norm as in sparse subspace clustering (SSC) [10], nuclear norm as in low-rank representation (LRR) [11], or a combination of these and other norms. An affinity/similarity matrix is then obtained as $|Z| + |Z|^T$, after which spectral clustering is performed. Other terms are considered in the optimization problem to provide robustness to noise and outliers, and numerous recent papers follow this framework [12], [13], [14], [15]. Efficient solutions to this problem based on orthogonal matching pursuit and elastic-net are presented in [16], [17]. Other approaches include thresholded subspace clustering (TSC) [18], in which an affinity matrix is formed by finding nearest neighbors of points in terms of spherical distance, and greedy subspace clustering (GSC) [19], which greedily builds subspaces in order to form an affinity matrix. In all cases, spectral clustering is performed as the final step to obtain cluster labels.

In contrast to the above methods, KSS seeks to minimize the sum of residuals of points to their assigned subspace, *i.e.*,

$$\min_{\mathcal{C}, \mathcal{U}} \sum_{k=1}^K \sum_{i: x_i \in c_k} \|x_i - U_k U_k^T x_i\|_2^2, \quad (1)$$

where $\mathcal{C} = \{c_1, \dots, c_K\}$ denotes the set of estimated clusters and $\mathcal{U} = \{U_1, \dots, U_K\}$ denotes the corresponding set of subspace bases. Beginning with an initialization of K candidate subspace bases, KSS proceeds in an alternating fashion by (i) clustering points via nearest subspace and (ii) obtaining new subspace bases by performing PCA on the points in each cluster. The algorithm is computationally efficient and guaranteed to converge to a local minimum [6], [7]. As with K -means, the KSS output is highly dependent on initialization. It is typically applied by performing many restarts and choosing the result with minimum cost (1) as the output. This idea was extended to minimize the ℓ_1 norm in [20], where a method for intelligent initialization is also proposed. In [21], the authors use an alternating method based on KSS to perform online subspace clustering in the case of missing data. Most recently, in [22], the authors propose a novel initialization method based on ideas from [23], and then perform the subspace update step using gradient steps along the Grassmann manifold. While this method is computationally efficient and improves upon the previous performance of KSS, it lacks theoretical guarantees.

Ensemble methods have been used in the context of general clustering for some time and fall within the domain of *consensus clustering*, with an overview of the benefits and techniques given in [24]. The central idea behind these methods is to obtain many clusterings from a simple base clusterer, such as K -means, and then combine the results intelligently. In order to obtain different clustering results from each base clustering, diversity of some sort must be incorporated. This is typically done by obtaining bootstrap samples of the data as in [25], [26], subsampling the data to reduce computational complexity as in [27], or performing random projections of the data [28]. Alternatively, the authors of [29], [30] use the randomness in different initializations of K -means to obtain diversity, which is the approach we take here for subspace clustering. After diversity is achieved, the base clustering results must be combined. The *evidence accumulation clustering* framework is laid out in [9], in which results are combined by voting, *i.e.*, creating a co-association matrix A whose (i, j) th entry is equal to the number of times two points are clustered together. A theoretical framework for this approach is laid out in [31], where the entries of the co-association matrix are modeled as Binomial random variables. This approach is studied further in [32], [33], in which the clustering problem is solved as a Bregman divergence minimization. These models result in improved clustering performance over previous work but are not accompanied by any theoretical guarantees with regard to the resulting co-association matrix. Further, they are not specifically designed to consider the case where the data are generated from the UoS model.

In the remainder of this paper, we apply ideas from consensus clustering to the subspace clustering problem. We describe our ensemble KSS algorithm and its guarantees and demonstrate the algorithm's state-of-the-art performance on synthetic and several real datasets.

III. ENSEMBLE K -SUBSPACES ALGORITHM & GUARANTEES

In this section, we describe our method for subspace clustering using ensembles of the K -subspaces algorithm, which we refer to as Ensemble K -subspaces (EKSS).

EKSS leverages the fact that for several runs of KSS, each random initialization results in some partially correct clustering information. We therefore run several random initializations of KSS and form a co-association matrix using the results of each run, after which we apply spectral clustering. Our theoretical results imply that even if the data come from generative subspaces with arbitrary positioning, the algorithm outputs a perfect clustering, as long as the maximum subspace affinity (defined below in Eq. (2)) is bounded and the points are drawn uniformly from the true subspaces without noise. For noisy data, the final affinity matrix contains no false connections between points.

In more technical detail, our EKSS algorithm proceeds as follows. For each of $b = 1, \dots, B$ base clusterings, we obtain a cluster estimate $\mathcal{C}^{(b)}$ from a single run of KSS with a random initialization. For each b such that the points x_i and x_j are

Algorithm 1 ENSEMBLE \bar{K} -SUBSPACES (EKSS)

```

1: Input:  $\mathcal{X} = \{x_1, x_2, \dots, x_N\} \subset \mathbb{R}^D$ : data,  $\bar{K}$ : number of candidate subspaces,  $\bar{d}$ : candidate dimension,  $K$ : number of
   output clusters,  $q$ : threshold parameter,  $B$ : number of base clusterings,  $T$ : number of KSS iterations
2: Output:  $\mathcal{C} = \{c_1, \dots, c_K\}$ : clusters of  $\mathcal{X}$ 
3: for  $b = 1, \dots, B$  (in parallel) do
4:    $U_1, \dots, U_{\bar{K}} \stackrel{iid}{\sim} \text{Unif}(\text{St}(D, \bar{d}))$  Draw  $\bar{K}$  random subspace bases
5:    $c_k \leftarrow \left\{x \in \mathcal{X} : \forall j \ \|U_k^T x\|_2 \geq \|U_j^T x\|_2\right\}$  for  $k = 1, \dots, \bar{K}$  Cluster by projection
6:   for  $t = 1, \dots, T$  (in sequence) do
7:      $U_k \leftarrow \text{PCA}(c_k, \bar{d})$  for  $k = 1, \dots, \bar{K}$  Estimate subspaces
8:      $c_k \leftarrow \left\{x \in \mathcal{X} : \forall j \ \|U_k^T x\|_2 \geq \|U_j^T x\|_2\right\}$  for  $k = 1, \dots, \bar{K}$  Cluster by projection
9:   end for
10:   $\mathcal{C}^{(b)} \leftarrow \{c_1, \dots, c_{\bar{K}}\}$ 
11: end for
12:  $A_{i,j} \leftarrow \frac{1}{B} |\{b : x_i, x_j \text{ are co-clustered in } \mathcal{C}^{(b)}\}|$  for  $i, j = 1, \dots, N$  Form affinity matrix
13:  $\bar{A} \leftarrow \text{THRESH}(A, q)$  Keep top  $q$  entries per row/column
14:  $\mathcal{C} \leftarrow \text{SPECTRALCLUSTERING}(\bar{A}, K)$  Final Clustering

```

clustered together, we add one to the (i, j) th entry of the co-association matrix. We then threshold the co-association matrix as in [18] by taking the top q values from each row/column. Once this thresholded co-association matrix is formed, cluster labels are obtained using spectral clustering. Pseudocode for EKSS is given in Alg. 1, where THRESH sets all but the top q entries in each row/column to zero as in [18] (pseudocode for this procedure is given in Appendix C) and SPECTRALCLUSTERING [34] clusters the data points based on the co-association matrix A . Note that the number of candidates \bar{K} and candidate dimension \bar{d} need not match the number K and dimension of the true underlying subspaces. Fig. 1 shows the progression of the co-association matrix as $B = 1, 5, 50$ base clusterings are used, in the case of noiseless data from $K = 4$ subspaces of dimension $d = 10$ in ambient space of dimension $D = 100$ using $\bar{K} = 4$ candidates of dimension $\bar{d} = 10$.

A. Recovery Guarantees

Recovery guarantees for KSS are still absent despite nearly twenty years of use since its introduction. Intelligent initialization methods based on probabilistic farthest insertion are provided in [20], [22], but these still lack any theoretical guarantees. In this section, we provide a first step toward understanding the performance of KSS, as well as recovery guarantees for the subspace clustering problem. We show that by combining the clusterings that result from many random initializations of subspace candidates, the entries of the resulting affinity matrix converge to a monotonically increasing function of the absolute value of inner product between points. A corollary of this fact is that a simplified version of EKSS exhibits all the recovery guarantees of TSC [18]. To the best of our knowledge, our work is the first to provide any theoretical guarantees for the KSS algorithm as well as the first characterization of the co-association matrix in the context of consensus clustering.

Due to its alternating nature, analyzing multiple iterations of the KSS algorithm remains challenging. Instead, we analyze the first iteration of KSS ($T = 0$ in Alg. 1), in which random candidates are drawn and points are clustered based on their nearest candidate. Further, we restrict ourselves to the case where the number of candidates (*not* the number of subspaces) is $\bar{K} = 2$ and the candidate dimension (*not* the true subspace dimension) is $\bar{d} = 1$. Finally, for the purposes of analysis, we replace the unit norm candidates in Step 4 with Gaussian random vectors, noting that the two are nearly equivalent in high dimensions due to concentration of the norm [35, Thm. 3.1.1]. We refer to EKSS with this choice of parameters as EKSS-0 and include explicit pseudocode in Appendix A. Remarkably, we show that combining the results from many random instances of this naïve algorithm leads to the same recovery guarantees as TSC, which are in turn comparable to those for SSC. While we do not analyze the case where multiple KSS iterations are performed, these iterations are guaranteed not to increase the KSS cost function, and in practice, we find that running KSS to convergence only improves clustering performance.

We now state our main result, which guarantees that EKSS-0 described in the preceding paragraph is able to cluster the points in \mathcal{X} exactly under given conditions on the maximum affinity between subspaces and the number of points per subspace. This result matches that of TSC [18, Thm. 2] exactly, and our proof leverages the proof of that used in [18] by applying Lemma 1 below. Our guarantees depend on the affinity between two subspaces, defined as [18], [36]

$$\text{aff}(\mathcal{S}_k, \mathcal{S}_l) = \frac{1}{\sqrt{d_k \wedge d_l}} \|U_k^T U_l\|_F, \quad (2)$$

where \mathcal{S}_k and \mathcal{S}_l are d_k - and d_l -dimensional subspaces with orthonormal bases U_k and U_l . Note that $\text{aff}(\mathcal{S}_k, \mathcal{S}_l)$ is a measure of how close two subspaces are in terms of their principal angles and takes the value 1 if two subspaces are equivalent and 0 if they are orthogonal.

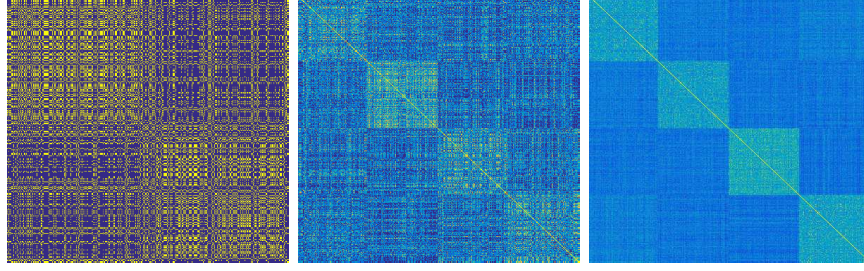


Fig. 1: Co-association matrix of EKSS for $B = 1, 5, 50$ base clusterings. Data generation parameters are $D = 100$, $d = 10$, $K = 4$, $N = 400$, and the data is noise-free; the algorithm uses $\bar{K} = 4$ candidate subspaces of dimension $\bar{d} = 10$. Resulting clustering errors are 54%, 25%, and 0%.

Theorem 1. Let \mathcal{S}_k , $k = 1, \dots, K$ be subspaces of dimension d_1, \dots, d_K in \mathbb{R}^D . Let the points in \mathcal{X}_k be a set of N_k points drawn uniformly from the unit sphere in subspace k , i.e., from the set $\{x \in \mathcal{S}_k : \|x\| = 1\}$. Let $\mathcal{X} = \mathcal{X}_1 \cup \dots \cup \mathcal{X}_K$ and $N = \sum_k N_k$. Let $q \in [c_1 \log N_{\max}, N_{\min}/6]$, where $N_{\min} = \min_k \{N_k\}$, $N_{\max} = \max_k \{N_k\}$, $c_1 = 18(12\pi)^{d-1}$, and $d = \max\{d_1, \dots, d_K\}$. If

$$\max_{k,l:k \neq l} \text{aff}(\mathcal{S}_k, \mathcal{S}_l) \leq \frac{1}{15 \log N},$$

then in the limit as $B \rightarrow \infty$, EKSS-0 delivers the correct clustering of \mathcal{X} with probability at least $1 - 10/N - \sum_{k=1}^K (N_k e^{-c(N_k-1)} + 2N_k^{-2})$, where $c > 0$ is a numerical constant.

Proof of Theorem 1. The proof hinges on the following lemma, which states that in the case where $T = 0$, $\bar{d} = 1$, and $\bar{K} = 2$, points x_i and x_j are clustered together with probability that increases monotonically with $|x_i^T x_j|$.

Lemma 1. The probability that two points $x_i, x_j \in \mathcal{X}$ are clustered together by one base clustering of EKSS-0 (i.e., EKSS-0 with $B = 1$) is an increasing function of $|x_i^T x_j|$.

The proof of Lemma 1 is given in Appendix A. By the Law of Large Numbers, when $B \rightarrow \infty$, each entry $A_{i,j}$ of the affinity matrix A approaches the probability analyzed in Lemma 1, and hence is also an increasing function of $|x_i^T x_j|$. Next, note that the result of [18, Thm. 2] depends only on the relative order of $|x_i^T x_j|$ (namely, through [18, Lemma 1] and [18, Lemma 2]). By Lemma 1, the order of entries in A is the same as in TSC, and so (as $B \rightarrow \infty$) the thresholded affinity matrix \bar{A} of EKSS-0 has the same connectivity as that formed by TSC [18]. The result of the theorem follows directly by the proof of [18, Thm. 2]. \square

Thm. 1 states that perfect clustering of the data is guaranteed even in the case of intersecting subspaces, as long as the subspaces are not too close in all directions. The clustering condition for Thm. 1 above is the same as that for SSC in [12] up to constants and log factors. Along with the above result, all recovery guarantees of TSC follow from Lemma 1, indicating that EKSS-0 results in no false connections under noisy data, missing data, and outliers. For a discussion of these guarantees and their relation to those for SSC and other algorithms, see [18, Sec. VII]. The inverse dependence on $\log N$ implies that the subspace affinity must shrink as N grows. On one hand, this is intuitive because with many points per subspace, it is likely that some points will be close to the intersection of two subspaces and potentially be misclustered. On the other hand, more points allows for a better chance that the nearest point by inner product is within the same subspace. Indeed, in all the empirical results we see that both EKSS and TSC perform better with larger N . Finally, we note that while the above analysis holds only for the case of $T = 0$, letting $T > 0$ is guaranteed not to increase the KSS cost function [6]. The extension of Thm. 1 to the case where $T > 0$ is an important topic of our ongoing research.

B. Implementation Details

In this section, we explain a few relevant implementation details, including a warm start extension of EKSS that we will show outperforms state-of-the-art methods on several benchmark datasets.

A natural heuristic to improve the clustering performance of EKSS is to add larger values to the affinity matrix for base clusterings in which the clustering is believed to be more accurate, and smaller values in the case where the clustering is believed to be more inaccurate. Here, we briefly describe one such approach. Note that Step 12 in EKSS is equivalent to setting $A \leftarrow \frac{1}{B} \sum_{b=1}^B A^{(b)} \phi(b)$, where $A_{i,j}^{(b)} := \mathbb{1}\{x_i, x_j \text{ are clustered together in } \mathcal{C}^{(b)}\}$ and $\phi(b) = 1$. One measure of clustering accuracy is the cost function of KSS with the clusters and subspace bases set as the clustering output. Let

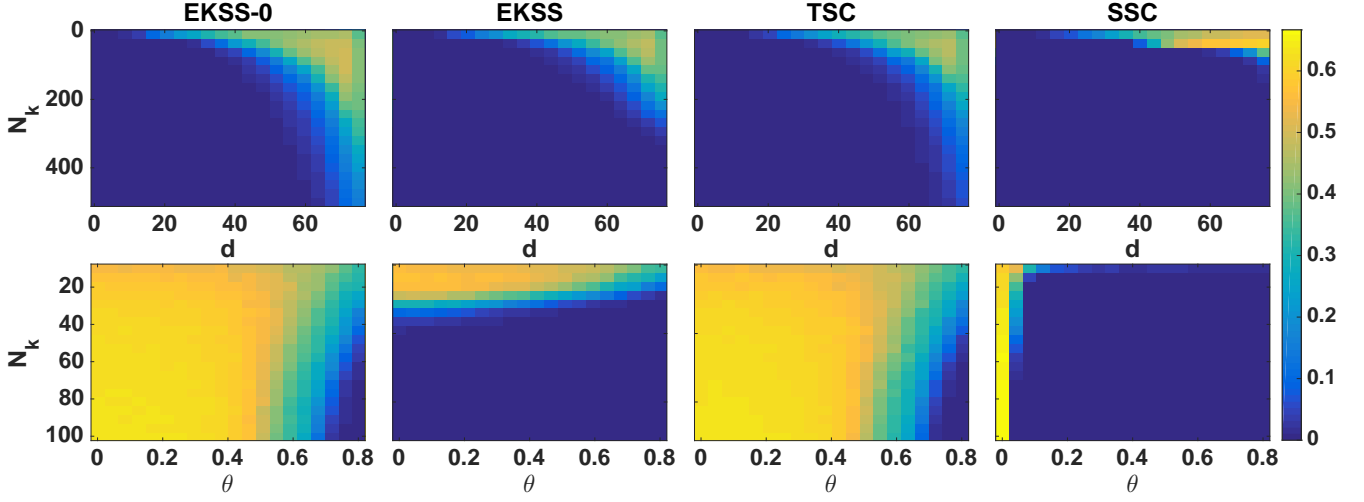


Fig. 2: Clustering error for proposed and state-of-the-art subspace clustering algorithms as a function of problem parameters N_k , number of points per subspace, and true subspace dimension d or angle between subspaces θ . Fixed problem parameters are $D = 100$, $K = 3$.

$\mathcal{C}^{(b)} = \{c_1^{(b)}, \dots, c_K^{(b)}\}$, and let $\mathcal{U}^{(b)} = \{U_1^{(b)}, \dots, U_K^{(b)}\}$ denote the set of subspace bases estimated by performing PCA on the points in the corresponding clusters. The clustering confidence can then be measured as

$$\phi(b) = 1 - \sum_{k=1}^K \sum_{i: x_i \in c_k^{(b)}} \left\| x_i - U_k^{(b)} U_k^{(b)T} x_i \right\|_2^2 / \|X\|_F^2, \quad (3)$$

a value between 0 and 1 that decreases as the KSS cost increases. We employ this value of $\phi(b)$ in all experiments on real data.

1) *Warm-Start EKSS*: It is well-known that the performance of alternating methods in optimization depends on the initialization of the problem parameters [37], [38]. For this reason, we propose a warm-start method to further improve robustness to outliers and noise. We first run EKSS with a small number of base clusterings (typically 10). Then, using the estimated labels obtained from this run, we form a set of initial candidate subspace bases by performing PCA on the points in each cluster. These candidate bases are then used to initialize KSS in place of random candidates for each $b = 1, \dots, B$ in EKSS. We refer to this variant as EKSS-WS (warm-start), and pseudocode for this algorithm is given in Appendix C.

2) *Parameter Selection*: In all experiments using EKSS, we take $\bar{K} = K$ and choose \bar{d} as the best approximation of the true subspace dimension. We assume in this work that a good approximating dimension for the underlying subspace is known, which is reasonable in several practical applications. For example, images of a Lambertian object under varying illumination are known to lie near a subspace with $d = 9$ [1] and moving objects in video are known to lie near an affine subspace with $d = 3$ [39]. In the case of unknown subspace dimensions, one could use EKSS with increasing \bar{d} , or methods such as those proposed in [8] could be employed.

Rather than choosing T explicitly in Alg. 1, we run KSS to convergence. The EKSS algorithm then relies on the appropriate choice of the number of base clusterings B and the thresholding parameter q . In general, B may be chosen as large as computation time allows. In our experiments on real data, we choose $B = 1000$. The thresholding parameter q can be chosen according to data-driven techniques as in [40], or following the choice in [18]. In our experiments on real data, we select the best q in a large range of values for each EKSS and TSC to provide a fair comparison. For the warm-start run of EKSS-WS, both B and q should be small (we choose $B = 10$ and $q = 3$). For comparison, TSC requires the choice of q , and SSC [10] and its variants [16], [17] all require two parameters to be selected. Finally, we use the implementation of SPECTRALCLUSTERING from [10].

IV. EXPERIMENTAL RESULTS

In this section, we demonstrate the performance in terms of clustering error (defined in Appendix C) of EKSS on both synthetic and real datasets. We first show the performance of our algorithm as a function of the relevant problem parameters and verify that EKSS-0 exhibits the same empirical performance as TSC. We also show that EKSS can recover subspaces that either have large intersection or are extremely close. We then demonstrate on real datasets that EKSS not only improves over previous iterative methods, but that the warm-start variant of EKSS surpasses state-of-the-art results in many cases.

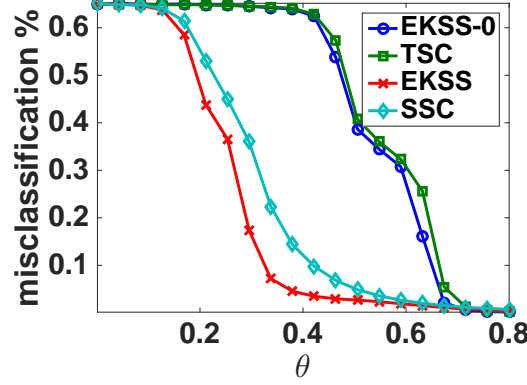


Fig. 3: Clustering error as a function of subspace angles with noisy data. Problem parameters are $D = 100$, $d = 10$, $K = 3$, $N_k = 500$, $\sigma^2 = 0.05$.

A. Synthetic Data

For all experiments in this section, we take $q = \max(3, \lceil N_k/20 \rceil)$ for EKSS-0 and TSC and $q = \max(3, \lceil N_k/6 \rceil)$ for EKSS, where $\lceil c \rceil$ denotes the largest integer greater than or equal to c . We set $B = 10,000$ for EKSS-0 and EKSS. To validate our theoretical results, we draw Gaussian candidates, rather than orthonormal bases, for EKSS-0. When the angles between subspaces are not explicitly specified, it is assumed that the subspaces are drawn uniformly at random from the set of all d -dimensional subspaces of \mathbb{R}^D . For all experiments, we draw points uniformly at random from the unit sphere in the corresponding subspace and show the mean error over 100 random problem instances. We use the code provided by the authors for TSC and SSC. We employ the ADMM implementation of SSC and choose the parameters that result in the best performance in each scenario.

We explore the influence of some relevant problem parameters on the EKSS algorithm in Fig. 2. We take the ambient dimension to be $D = 100$, the number of subspaces to be $K = 3$, and assume the data to be noiseless.

We first explore the dependence on subspace dimension and the number of points per subspace. The top row of Fig. 2 shows the misclassification rate as the number of points per subspace ranges from 10 – 500 and the subspace dimension ranges from 1 – 75. When $2d > D$ ($d = 51$ in this case), pairs of subspaces necessarily have intersection, and the intersection dimension grows with d . First, the figures demonstrate that EKSS-0 achieves roughly the same performance as TSC, resulting in correct clustering even in the case of subspaces with large intersection. Second, we see that EKSS can correctly cluster for subspace dimensions larger than that of TSC as long as there are sufficiently many points per subspace. For large subspace dimensions with a moderate number of points per subspace, SSC achieves the best performance.

We next explore the clustering performance as a function of the distance between subspaces, as shown in the second row of Fig. 2. We set the subspace dimension to $d = 10$ and generate $K = 3$ subspaces such that all principal angles are θ , for 20 values in the range $[0.001, 0.8]$. Most strikingly, EKSS is able to resolve subspaces with even the smallest separation. This stands in contrast to TSC, which fails in this regime because when the subspaces are extremely close, the inner products between points on different subspaces can be nearly as large as those within the same subspace. Similarly, in the case of SSC, points on a different subspace can be used to regress any given point without any added cost, and so it fails at very small subspace angles. However, as long as there is still some separation between subspaces, EKSS is able to correctly cluster all points. While the theory presented here does not capture this phenomenon, recovery guarantees that take into account multiple iterations of KSS are an important topic for future work.

As a final comparison, we show the clustering performance with noisy data. Fig. 3 shows the clustering error as a function of the angle between subspaces for the case of $K = 3$ subspaces of dimension $d = 10$, with $N_k = 500$ points corrupted by zero-mean Gaussian noise with covariance $0.05I_D$. The figure shows again that EKSS-0 and TSC obtain similar performance, and more importantly that EKSS is more robust to small subspace angles than SSC, even in the case of noisy data.

B. Real Data

In this section, we show that EKSS achieves competitive performance on a variety of real datasets commonly used as benchmarks in the subspace clustering literature. We consider the Hopkins-155 dataset [2], the cropped Extended Yale Face Database B [4], [42], COIL-20 [43] and COIL-100 [44] object databases, the USPS dataset provided by [45], and 10,000 digits of the MNIST handwritten digit database [5], where we obtain features using a scattering network [46] as in [17]. Descriptions of these datasets and the relevant problem parameters are included in Appendix C. For the Hopkins-155 database, we report both the mean and median misclassification rates, as is common in the literature [10], [22]. We compare the performance of EKSS to several benchmark algorithms: KSS [6], Median K-Flats (MKF) [20], TSC [18], SSC-OMP [16], Elastic Net

Algorithm	Hopkins	Yale B	COIL-20	COIL-100	USPS	MNIST-10k
EKSS	5.84/0.32	22.33	24.79	36.36	33.21	26.18
EKSS-WS	3.82/0.00	16.12	7.01	28.03	26.09	17.54
KSS	7.00/0.79	75.70	65.56	74.53	51.30	48.15
MKF	5.22/0.21	47.70	54.79	66.49	28.62	47.14
TSC	27.19/27.27	20.81	15.35	39.03	33.46	17.17
SSC-ADMM	2.18/0.00	31.03	22.43	44.06	56.61	19.17
SSC-OMP	35.77/36.65	22.41	46.67	62.12	78.43	19.47
EnSC	24.96/24.21	21.26	15.14	28.75	33.66	17.97
OLRSC	20.70/18.12	55.14	35.42	50.79	29.71	20.50

TABLE I: Clustering error of subspace clustering algorithms for a variety of benchmark datasets. Hopkins-155 performance is (mean/median). The lowest two clustering errors are given in bold.

Subspace Clustering (EnSC) [17], and Online Low-Rank Subspace Clustering (OLRSC) [15]. For EKSS we use $B = 1000$ base clusterings. For all others but KSS, we use the code provided by the authors and use the recommended parameters where available and otherwise use parameters that result in the best performance. For a fair comparison to KSS and MKF, we run 1000 trials of each and use the clustering result that achieves the lowest KSS cost. We refer to the warm-start variant of EKSS as EKSS-WS. Further implementation details, including parameter selection and data preprocessing, can be found in Appendix C.

The clustering error for all datasets and algorithms is shown in Table I, with the lowest two errors given in bold. First, note that EKSS outperforms KSS in all cases, and typically by a very large margin. This result emphasizes the importance of leveraging all clustering information from the B base clusterings, as opposed to simply choosing the best single clustering. Next, the results show that EKSS-WS is among the top two performers in all datasets considered. Although code for the method from [22] was unavailable, EKSS-WS achieves similar performance to the reported misclassification rate on the Hopkins-155 dataset. We also observe that scalable algorithms such as SSC-OMP and EnSC perform poorly on the Hopkins dataset, likely due to the small number of points, whereas EKSS works well under both small and large N . Most striking are the resulting misclassification rates on the Yale B and COIL-20 datasets, for which EKSS-WS significantly outperforms the best existing algorithm. Interestingly, TSC achieves the best performance on the MNIST-10k dataset, whereas EnSC achieves much better performance on the full 70,000-digit database as reported in [17]. Due to memory constraints we were unable to compare performance on the full MNIST database for most algorithms including EKSS. Implementing a memory-efficient version of EKSS is an important topic of future work.

V. CONCLUSION

In this work, we presented a first step toward a theoretical understanding of the KSS algorithm by analyzing the effect of combining multiple clusterings using the evidence accumulation clustering framework. We showed that with a given choice of parameters, our algorithm can provably cluster data from a union of subspaces under the same conditions as existing algorithms. We demonstrated the efficacy of our approach on both synthetic and real data, and showed that a warm-start variant of our method achieves excellent performance on several real datasets.

While the theoretical guarantees presented here match existing guarantees in the literature, our experiments on synthetic data indicate that the iterative approach of KSS provides a major improvement in robustness to small angles between subspaces. Further, while our results hold only for the case of two 1-dimensional candidates, we observed a performance improvement in the case where more than two d -dimensional candidates are used. Extending our analysis to the general case of Alg. 1 (e.g., $T > 0$, $\bar{d} > 1$, and $\bar{K} > 2$) is an important next step. Finally, while EKSS-WS with the given parameter choices achieves excellent empirical performance, a deeper understanding of appropriate parameter selection for this method could lead to improved performance and robustness across different datasets.

Algorithm 2 EKSS-0

```

1: Input:  $\mathcal{X} = \{x_1, x_2, \dots, x_N\} \subset \mathbb{R}^D$ : data,  $K$ : number of output clusters,  $q \in \mathbb{N}$ : threshold parameter,  $B$ : number of base
   clusterings
2: Output:  $\mathcal{C} = \{c_1, \dots, c_K\}$ : clusters of  $\mathcal{X}$ 
3: for  $b = 1, \dots, B$  (in parallel) do
4:    $u_1, u_2 \sim \mathcal{N}(0, \frac{1}{D}I_D)$  Draw two random candidates
5:    $c_k \leftarrow \{x \in \mathcal{X} : |u_k^T x| \geq |u_l^T x|\} \text{ for } k, l = 1, 2$  Cluster by inner product
6:    $\mathcal{C}^{(b)} \leftarrow \{c_1, c_2\}$ 
7: end for
8:  $A_{i,j} \leftarrow \frac{1}{B} |\{b : x_i, x_j \text{ are clustered together in } \mathcal{C}^{(b)}\}| \text{ for } i, j = 1, \dots, N$  Form affinity matrix
9:  $\bar{A} \leftarrow \text{THRESH}(A, q)$  Threshold
10:  $\mathcal{C} \leftarrow \text{SPECTRALCLUSTERING}(\bar{A}, K)$  Final Clustering

```

APPENDIX A
PROOF OF LEMMA 1

In this section, we prove Lemma 1 of Section III-A, which allows us to leverage the connectivity results for TSC [18] in Theorem 1. For convenience, we include pseudocode for the explicit EKSS-0 algorithm in Alg. 2 and restate the lemma below.

Lemma 1. *The probability that two points $x_i, x_j \in \mathcal{X}$ are clustered together by one base clustering of EKSS-0 (i.e., EKSS-0 with $B = 1$) is an increasing function of $|x_i^T x_j|$.*

Proof. Let $u, v \sim \mathcal{N}(0, \frac{1}{D}I_D)$ be two one-dimensional Gaussian candidates in EKSS-0. Then u and v are orthogonally invariant, i.e., $Qu, Qv \sim \mathcal{N}(0, \frac{1}{D}I_D)$ for any orthogonal matrix Q . Furthermore, x and y cluster together if and only if x and $-y$ cluster together. As a result, we can consider $x = [1 \ 0 \ \dots \ 0]^T$ and $y = [\cos \theta \ \sin \theta \ 0 \ \dots \ 0]^T$ where $0 < \theta < \pi/2$ without loss of generality. The points x and y are clustered together when

$$(|u_1| > |v_1| \text{ and } |u_1 \cos \theta + u_2 \sin \theta| > |v_1 \cos \theta + v_2 \sin \theta|) \quad (4)$$

or

$$(|u_1| < |v_1| \text{ and } |u_1 \cos \theta + u_2 \sin \theta| < |v_1 \cos \theta + v_2 \sin \theta|). \quad (5)$$

Note that (4) and (5) are disjoint events and occur with equal probability since u and v are identically distributed. The remainder of the proof is dedicated to showing that the conditional probability of (4) given u_1 and v_1 is a decreasing function of θ when $|u_1| > |v_1|$. From this fact, it follows that the probability of (4) is a decreasing function of θ by the law of total probability (taken over u_1 and v_1). Lemma 1 follows then because (5) has equal probability and $\theta = \arccos(|x^T y|)$ is a decreasing function of $|x^T y|$.

Observe that

$$|u_1| > |v_1| \iff \underbrace{[(u_1 + v_1 > 0 \text{ and } u_1 - v_1 > 0)]}_{\text{i.e., } u_1 > |v_1|} \text{ or } \underbrace{[(u_1 + v_1 < 0 \text{ and } u_1 - v_1 < 0)]}_{\text{i.e., } u_1 < -|v_1|} \quad (6)$$

and likewise

$$|u_1 \cos \theta + u_2 \sin \theta| > |v_1 \cos \theta + v_2 \sin \theta| \quad (7)$$

\iff

$$(u_2 + v_2 > -(u_1 + v_1) \cot \theta \text{ and } u_2 - v_2 > -(u_1 - v_1) \cot \theta) \quad (8)$$

$$\text{or } (u_2 + v_2 < -(u_1 + v_1) \cot \theta \text{ and } u_2 - v_2 < -(u_1 - v_1) \cot \theta). \quad (9)$$

For convenience, let $s_1 = u_1 + v_1$, $d_1 = u_1 - v_1$, $s_2 = u_2 + v_2$ and $d_2 = u_2 - v_2$. The random variables s_2 and d_2 are i.i.d. Gaussian random variables because the vector $[s_2 \ d_2]^T$ is a scaled rotation of $[u_2 \ v_2]^T$ and u_2 and v_2 are i.i.d. Gaussian random variables. From (6) and (7), it follows that when $|u_1| > |v_1|$, either $s_1, d_1 > 0$ or $s_1, d_1 < 0$ and the conditional probability of (4) given u_1 and v_1 is

$$\begin{aligned}
\rho(\theta) &= \mathbb{P}\{|u_1| > |v_1| \text{ and } |u_1 \cos \theta + u_2 \sin \theta| > |v_1 \cos \theta + v_2 \sin \theta| : u_1, v_1\} \\
&= \mathbb{P}\{|u_1 \cos \theta + u_2 \sin \theta| > |v_1 \cos \theta + v_2 \sin \theta| : u_1, v_1\} \\
&= \mathbb{P}\{(s_2 > -s_1 \cot \theta \text{ and } d_2 > -d_1 \cot \theta) \text{ or } (s_2 < -s_1 \cot \theta \text{ and } d_2 < -d_1 \cot \theta) : s_1, d_1\} \\
&= \mathbb{P}\{s_2 > -s_1 \cot \theta : s_1\} \mathbb{P}\{d_2 > -d_1 \cot \theta : d_1\} + \mathbb{P}\{s_2 < -s_1 \cot \theta : s_1\} \times \\
&\quad \mathbb{P}\{d_2 < -d_1 \cot \theta : d_1\} \\
&= (1 - F(-s_1 \cot \theta))(1 - F(-d_1 \cot \theta)) + F(-s_1 \cot \theta)F(-d_1 \cot \theta)
\end{aligned} \quad (10)$$

where $F(x) = \int_{-\infty}^x f(\tau)d\tau$ is the CDF for the i.i.d. Gaussian random variables u_2 and v_2 with density $f(x)$. Differentiating (10) with respect to θ and factoring yields

$$\rho'(\theta) = -\underbrace{\csc^2 \theta}_{>0} \left[\underbrace{f(-d_1 \cot \theta)}_{>0} \underbrace{d_1(1 - 2F(-s_1 \cot \theta))}_{=: \delta_1} + \underbrace{f(-s_1 \cot \theta)}_{>0} \underbrace{s_1(1 - 2F(-d_1 \cot \theta))}_{=: \delta_2} \right]$$

Recall that either $s_1, d_1 > 0$ or $s_1, d_1 < 0$. We consider each case:

- 1) If $s_1, d_1 > 0$ then $F(-s_1 \cot \theta), F(-d_1 \cot \theta) \leq 1/2$ with equality only when $\theta = \pi/2$. As a result $\delta_1, \delta_2 \geq 0$ with equality only when $\theta = \pi/2$.
- 2) If $s_1, d_1 < 0$ then $F(-s_1 \cot \theta), F(-d_1 \cot \theta) \geq 1/2$ with equality only when $\theta = \pi/2$. Once again $\delta_1, \delta_2 \geq 0$ with equality only when $\theta = \pi/2$.

Thus it follows that $\rho'(\theta) \leq 0$ with equality only when $\theta = \pi/2$ and so the conditional probability $\rho(\theta)$ of (4) given u_1 and v_1 is a decreasing function of θ when $|u_1| > |v_1|$. \square

APPENDIX B NON-GLOBAL CONVERGENCE OF K -SUBSPACES

In this section, we prove the claim that there is a set of initializations of nonzero measure that will necessarily lead the K -subspaces (KSS) algorithm to a solution that is not a global minimizer for the simple case of two one-dimensional subspaces of \mathbb{R}^2 .

Proposition 1. *Consider two one-dimensional subspaces $\mathcal{S}_1, \mathcal{S}_2 \subset \mathbb{R}^2$ having angle between them $\theta \in (0, \pi/2)$. The set of initializations such that KSS converges to a clustering that is not a global optimum has nonzero measure.*

Proof. Let u_1, u_2 be the true subspace bases, and let v_1, v_2 be the candidate bases initialized uniformly at random from the unit sphere. Let $\theta_{u,v}$ denote the angle between vectors u and v , i.e., $\theta_{u,v} = \cos^{-1}(u^T v)$, where by symmetry we only consider angles at most $\pi/2$. By rotation invariance of the candidate subspaces, we assume that $u_1 = [1 \ 0]^T$ and $u_2 = [\cos(\theta) \ \sin(\theta)]^T$ without loss of generality. Consider the case where $\theta_{u_1, v_1} > \theta$ and $\theta_{u_1, v_2} > \theta$, and note that each event occurs independently with probability $\pi/2 - \theta$. Next, note that $\theta_{u_2, v_1} < \theta_{u_2, v_2}$ implies $\theta_{u_1, v_1} < \theta_{u_1, v_2}$, in which case all points are assigned to v_1 . Similarly, $\theta_{u_2, v_2} < \theta_{u_2, v_1}$ implies $\theta_{u_1, v_2} < \theta_{u_1, v_1}$, in which case all points are assigned to v_2 . Thus, all points are clustered to the same candidate subspace as long as both $\theta_{u_1, v_1} > \theta$ and $\theta_{u_1, v_2} > \theta$, which occurs with probability $(\pi/2 - \theta)^2$. Under this event, KSS converges after the first iteration, as the subspace corresponding one candidate is null. Hence, the set of initializations such that KSS converges to a local and not global optimum has measure at least $(\pi/2 - \theta)^2$. \square

APPENDIX C IMPLEMENTATION DETAILS

In this section, we include implementation details beyond those included in Section III-B. We first provide pseudocode for the THRESH and EKSS-WS algorithms. We then describe all preprocessing steps and parameters used for our experiments on real data.

A. Clustering Error

The clustering error, which is the metric used for all experimental results, is computed by matching the true labels and the labels output by a given clustering algorithm,

$$\text{err} = 100 \left(1 - \max_{\pi} \frac{1}{N} \sum_{i,j} Q_{\pi(i)j}^{\text{out}} Q_{ij}^{\text{true}} \right),$$

where π is a permutation of the cluster labels, and Q^{out} and Q^{true} are the output and ground-truth labelings of the data, respectively, where the (i, j) th entry is one if point j belongs to cluster i and is zero otherwise.

B. Pseudocode

In Algorithm 3 is the pseudocode for the THRESH routine used in the EKSS algorithm, which results in the same connectivity as thresholding in TSC [18].

Algorithm 3 AFFINITY THRESHOLD (THRESH)

```

1: Input:  $A \in [0, 1]^{N \times N}$ : affinity matrix,  $q$ : threshold parameter
2: Output:  $\bar{A} \in [0, 1]^{N \times N}$ : thresholded affinity matrix
3: for  $i = 1, \dots, N$  do
4:    $Z_{i,:}^{\text{row}} \leftarrow A_{i,:}$  with the smallest  $N - q$  entries set to zero.           Threshold rows
5:    $Z_{:,i}^{\text{col}} \leftarrow A_{:,i}$  with the smallest  $N - q$  entries set to zero.       Threshold columns
6: end for
7:  $\bar{A} \leftarrow \frac{1}{2} (Z^{\text{row}} + Z^{\text{col}})$                                            Average

```

Algorithm 4 EKSS WARM-START (EKSS-WS)

```

1: Input:  $\mathcal{X} = \{x_1, x_2, \dots, x_N\} \subset \mathbb{R}^D$ : data,  $\bar{K}$ : number of candidate subspaces,  $\bar{d}$ : candidate dimension,  $K$ : number of
   output clusters,  $q_1, q_2$ : threshold parameters,  $B_1, B_2$ : number of base clusterings,  $T$ : number of KSS iterations
2: Output:  $\mathcal{C} = \{c_1, \dots, c_K\}$ : clusters of  $\mathcal{X}$ 
3: for  $b = 1, \dots, B_1$  (in parallel) do
4:    $\{c_1, \dots, c_{\bar{K}}\} \leftarrow \text{EKSS}(\mathcal{X}, \bar{K}, \bar{d}, \bar{K}, q_2, B_2, T)$ 
5:   for  $t = 1, \dots, T$  (in sequence) do
6:      $U_k \leftarrow \text{PCA}(c_k, \bar{d})$  for  $k = 1, \dots, \bar{K}$                                Estimate subspaces
7:      $c_k \leftarrow \{x \in \mathcal{X} : \forall j \ \|U_k^T x\|_2 \geq \|U_j^T x\|_2\}$  for  $k = 1, \dots, \bar{K}$    Cluster by projection
8:   end for
9:    $\mathcal{C}^{(b)} \leftarrow \{c_1, \dots, c_{\bar{K}}\}$ 
10: end for
11:  $A_{i,j} \leftarrow \frac{1}{B_1} |\{b : x_i, x_j \text{ are clustered together in } \mathcal{C}^{(b)}\}|$  for  $i, j = 1, \dots, N$    Form affinity matrix
12:  $\bar{A} \leftarrow \text{THRESH}(A, q_1)$                                                          Keep top  $q_1$  entries per row/column
13:  $\mathcal{C} \leftarrow \text{SPECTRALCLUSTERING}(\bar{A}, K)$                                            Final Clustering

```

We also give in Algorithm 4 the pseudocode for EKSS-WS, which calls the EKSS algorithm given in Algorithm 1. Recall that the algorithm proceeds by first running EKSS for a small number of base clusterings (typically $B_2 \approx 10$). The output clustering is then used to initialize KSS for each of the B_1 base clusterings of the main loop.

C. Experiments on Real Data

In this section, we describe the real datasets used in our experiments, as well as any preprocessing steps and the parameters selected for all algorithms. All datasets are normalized so that each column lies on the unit sphere in the corresponding ambient dimension, as is common in the literature [12], [18], [22]. Table II gives a summary of all datasets considered.

The Hopkins-155 dataset [2] consists of 155 motion sequences with $K = 2$ in 120 of sequences and $K = 3$ in the remaining 35. In each sequence, objects moving along different trajectories each lie near their own affine subspace of dimension at most 3. We perform no preprocessing steps on this dataset.

The Extended Yale Face Database B [4], [42] consists of 64 images of each of 38 different subjects under a variety of lighting conditions. Each image is of nominal size 192×168 and is known to lie near a 9-dimensional subspace [1]. We downsample so that each image is of size 48×42 , as in [10]. For EKSS, EKSS-WS, KSS, MKF, TSC, and OLRSC, we perform an initial whitening as in [23], [18] by removing the first two singular components of the dataset and then project the data onto its first 500 principal components to reduce the computational complexity of these methods. Whitening resulted in worse performance for all other algorithms, so we omitted this step.

The COIL-20 [43] and COIL-100 [44] datasets consist of 72 images of 20 and 100 distinct objects (respectively) under a variety of rotations. All images are of size 32×32 . On both datasets, we whiten by removing the first singular component when it improves algorithm performance.

The USPS dataset provided by [45] contains 9,298 total handwritten digits of size 16×16 with roughly even label distribution. No preprocessing is performed on this dataset.

The MNIST dataset [5] contains a total of 70,000 handwritten digits, of which we consider only the 10,000 “test” images. The images have nominal size 28×28 , and we use the output of a scattering convolutional network [46] of size 3,472 and then project onto the first 500 principal components as in [17].

The parameters used for all experiments are shown in Table III. We use the recommended parameters where available and choose the parameters that result in the best performance in all other cases. For OLRSC [15], we use the recommended parameters, set the basis dimension as $K * d$, and report the minimum error between the standard and fully online pipelines, indicated by ‘S’ and ‘F’ in the table.

Dataset	N	K	D	d
Hopkins-155	39-556	2-3	30-200	3
Yale	2432	38	2016	9
COIL-20	1440	20	1024	9
COIL-100	7200	100	1024	9
USPS	9298	10	256	15
MNIST-10k	10000	10	500	3

TABLE II: Datasets used for experiments with relevant parameters; N : total number of samples, K : number of clusters, D : ambient dimension, d : estimated subspace dimension.

Algorithm	Hopkins	Yale	COIL-20	COIL-100	USPS	MNIST-10k
EKSS	$B = 1000, q = 15$	$B = 1000, q = 5$	$B = 1000, q = 35$	$B = 1000, q = 11$	$B = 1000, q = 7$	$B = 1000, q = 9$
EKSS-WS	$B_1 = 1000, q_1 = 15$ $B_2 = 10, q_2 = 3$	$B_1 = 1000, q_1 = 19$ $B_2 = 10, q_2 = 3$	$B_1 = 1000, q_1 = 50$ $B_2 = 10, q_2 = 3$	$B_1 = 1000, q_1 = 60$ $B_2 = 10, q_2 = 3$	$B_1 = 1000, q_1 = 500$ $B_2 = 10, q_2 = 3$	$B_1 = 1000, q_1 = 8$ $B_2 = 10, q_2 = 3$
TSC	$q = 3$	$q = 3$	$q = 8$	$q = 8$	$q = 5$	$q = 9$
SSC-ADMM	$\rho = 0.7, \alpha = 800$	$\rho = 1, \alpha = 20$	$\rho = 1, \alpha = 20$	$\rho = 1, \alpha = 20$	$\rho = 1, \alpha = 20$	$\rho = 1, \alpha = 20$
SSC-OMP	$\varepsilon = 2^{-52}, k_{max} = 3$	$\varepsilon = 2^{-52}, k_{max} = 5$	$\varepsilon = 2^{-52}, k_{max} = 5$	$\varepsilon = 2^{-52}, k_{max} = 5$	$\varepsilon = 2^{-52}, k_{max} = 5$	$\varepsilon = 2^{-52}, k_{max} = 12$
EnSC	$\lambda = 0.1, \alpha = 3$	$\lambda = 0.95, \alpha = 3$	$\lambda = 0.95, \alpha = 3$	$\lambda = 0.95, \alpha = 3$	$\lambda = 0.95, \alpha = 50$	$\lambda = 0.95, \alpha = 3$
OLRSC	F	S	F	F	F	F

TABLE III: Parameters used in experiments on real datasets for all algorithms considered.

REFERENCES

- [1] R. Basri and D. Jacobs, "Lambertian reflectance and linear subspaces," *IEEE TPAMI*, vol. 25, no. 2, pp. 218–233, February 2003.
- [2] R. Tron and R. Vidal, "A benchmark for the comparison of 3-D motion segmentation algorithms," in *IEEE Int. Conf. on Comp. Vision and Pattern Recog.*, 2011.
- [3] R. Vidal, S. S. Sastry, and Y. Ma, *Generalized Principal Component Analysis*. Springer-Verlag, 2016.
- [4] A. Georgiades, P. Belhumeur, and D. Kriegman, "From few to many: Illumination cone models for face recognition under variable lighting and pose," *IEEE Trans. Pattern Anal. Mach. Intelligence*, vol. 23, no. 6, pp. 643–660, 2001.
- [5] Y. LeCun, C. Cortes, and C. J. C. Burges, "The MNIST database of handwritten digits," 2016. [Online]. Available: yann.lecun.com/exdb/mnist
- [6] P. S. Bradley and O. L. Mangasarian, "k-Plane clustering," *Journal of Global Optimization*, vol. 16, pp. 23–32, 2000.
- [7] P. Tseng, "Nearest q-flat to m points," *Journal of Optimization Theory and Applications*, vol. 105, no. 1, pp. 249–252, 2000.
- [8] P. K. Agarwal and N. H. Mustafa, "K-means projective clustering," in *Proceedings of the twenty-third ACM SIGMOD-SIGACT-SIGART symposium on Principles of database systems*. ACM, 2004, pp. 155–165.
- [9] A. L. Fred and A. K. Jain, "Combining multiple clusterings using evidence accumulation," *IEEE transactions on pattern analysis and machine intelligence*, vol. 27, no. 6, pp. 835–850, 2005.
- [10] E. Elhamifar and R. Vidal, "Sparse subspace clustering: Algorithm, theory, and applications," *IEEE Trans. on Pattern Analysis and Machine Intelligence*, vol. 35, pp. 2765–2781, Nov. 2013.
- [11] G. Liu, Z. Lin, and Y. Yu, "Robust subspace segmentation by low-rank representation," in *Proceedings of the 27th international conference on machine learning (ICML-10)*, 2010, pp. 663–670.
- [12] M. Soltanolkotabi and E. J. Candes, "A Geometric Analysis of Subspace Clustering with Outliers," *The Annals of Statistics*, vol. 40, no. 4, pp. 2195–2238, 2012.
- [13] C.-Y. Lu, H. Min, Z.-Q. Zhao, L. Zhu, D.-S. Huang, and S. Yan, "Robust and efficient subspace segmentation via least squares regression," *Computer Vision–ECCV 2012*, pp. 347–360, 2012.
- [14] R. Vidal and P. Favaro, "Low rank subspace clustering (lsrc)," *Pattern Recognition Letters*, vol. 43, pp. 47–61, 2014.
- [15] J. Shen, P. Li, and H. Xu, "Online low-rank subspace clustering by basis dictionary pursuit," in *Proc. International Conference on Machine Learning*, 2016.
- [16] C. You, D. P. Robinson, and R. Vidal, "Scalable sparse subspace clustering by orthogonal matching pursuit," in *Proc. IEEE Conf. on Computer Vision and Pattern Recognition*, 2015.
- [17] C. You, C.-G. Li, D. P. Robinson, and R. Vidal, "Oracle based active set algorithm for scalable elastic net subspace clustering," *arXiv*, vol. 1605.02633v1, 2016.
- [18] R. Heckel and H. Bölcskei, "Robust subspace clustering via thresholding," *IEEE Trans. Inf. Theory*, vol. 24, no. 11, pp. 6320–6342, 2015.
- [19] D. Park, C. Caramanis, and S. Sanghavi, "Greedy subspace clustering," in *Advances in Neural Information Processing Systems*, 2014, pp. 2753–2761.
- [20] T. Zhang, A. Szlam, and G. Lerman, "Median k-flats for hybrid linear modeling with many outliers," in *Computer Vision Workshops (ICCV Workshops)*, 2009 *IEEE 12th International Conference on*. IEEE, 2009, pp. 234–241.
- [21] L. Balzano, A. Szlam, B. Recht, and R. Nowak, "K-Subspaces with missing data," in *Statistical Signal Processing Workshop (SSP), 2012 IEEE*. IEEE, 2012, pp. 612–615.
- [22] J. He, Y. Zhang, J. Wang, N. Zeng, and H. Hao, "Robust k-subspaces recovery with combinatorial initialization," in *Big Data (Big Data), 2016 IEEE International Conference on*. IEEE, 2016, pp. 3573–3582.
- [23] T. Zhang, A. Szlam, Y. Wang, and G. Lerman, "Hybrid linear modeling via local best-fit flats," *International Journal of Computer Vision*, vol. 100, pp. 217–240, 2012.
- [24] J. Ghosh and A. Acharya, "Cluster ensembles," *Wiley Interdisciplinary Reviews: Data Mining and Knowledge Discovery*, vol. 1, no. 4, pp. 305–315, 2011.
- [25] F. Leisch, "Bagged clustering," WU Vienna University of Economics and Business, Tech. Rep., 1999.
- [26] B. Minaei-Bidgoli, A. Topchy, and W. F. Punch, "Ensembles of partitions via data resampling," in *Information Technology: Coding and Computing, 2004. Proceedings. ITCC 2004. International Conference on*, vol. 2. IEEE, 2004, pp. 188–192.
- [27] K. Tumer and A. K. Agogino, "Ensemble clustering with voting active clusters," *Pattern Recognition Letters*, vol. 29, no. 14, pp. 1947–1953, 2008.
- [28] A. Topchy, A. K. Jain, and W. Punch, "Clustering ensembles: Models of consensus and weak partitions," *IEEE Transactions on pattern analysis and machine intelligence*, vol. 27, no. 12, pp. 1866–1881, 2005.
- [29] A. Fred and A. K. Jain, "Evidence accumulation clustering based on the k-means algorithm," in *Joint IAPR International Workshops on Statistical Techniques in Pattern Recognition (SPR) and Structural and Syntactic Pattern Recognition (SSPR)*. Springer, 2002, pp. 442–451.
- [30] A. L. Fred and A. K. Jain, "Data clustering using evidence accumulation," in *Pattern Recognition, 2002. Proceedings. 16th International Conference on*, vol. 4. IEEE, 2002, pp. 276–280.

- [31] S. R. Bulò, A. Lourenço, A. Fred, and M. Pelillo, "Pairwise probabilistic clustering using evidence accumulation," in *Joint IAPR International Workshops on Statistical Techniques in Pattern Recognition (SPR) and Structural and Syntactic Pattern Recognition (SSPR)*. Springer, 2010, pp. 395–404.
- [32] A. Lourenço, S. R. Bulò, N. Rebagliati, A. L. Fred, M. A. Figueiredo, and M. Pelillo, "Probabilistic evidence accumulation for clustering ensembles," in *ICPRAM*, 2013, pp. 58–67.
- [33] —, "Probabilistic consensus clustering using evidence accumulation," *Machine Learning*, vol. 98, no. 1-2, pp. 331–357, 2015.
- [34] A. Ng, Y. Weiss, and M. Jordan, "On spectral clustering: Analysis and an algorithm," in *Proc. Neural Information Processing Systems*, 2001.
- [35] R. Vershynin, *A Course in High Dimensional Probability*, 2016. [Online]. Available: www-personal.umich.edu/~romanv/teaching/2015-16/626/HDP-book.pdf
- [36] D. Zhang and L. Balzano, "Global convergence of a grassmannian gradient descent algorithm for subspace estimation," in *Proceedings of the 19th International Conference on Artificial Intelligence and Statistics*, ser. Proceedings of Machine Learning Research, A. Gretton and C. C. Robert, Eds., vol. 51. Cadiz, Spain: PMLR, 09–11 May 2016, pp. 1460–1468. [Online]. Available: <http://proceedings.mlr.press/v51/zhang16b.html>
- [37] D. Arthur and S. Vassilvitskii, "k-means++: The advantages of careful seeding," in *Proceedings of the eighteenth annual ACM-SIAM symposium on Discrete algorithms*. Society for Industrial and Applied Mathematics, 2007, pp. 1027–1035.
- [38] P. Jain, P. Netrapalli, and S. Sanghavi, "Low-rank matrix completion using alternating minimization," in *Proceedings of the forty-fifth annual ACM symposium on Theory of computing*. ACM, 2013, pp. 665–674.
- [39] C. Tomasi and T. Kanade, "Shape and motion from image streams under orthography," *Int'l J. Computer Vision*, vol. 9, no. 2, pp. 137–154, 1992.
- [40] R. Heckel, E. Agustsson, and H. Bolcskei, "Neighborhood selection for thresholding-based subspace clustering," in *Acoustics, Speech and Signal Processing (ICASSP), 2014 IEEE International Conference on*. IEEE, 2014, pp. 6761–6765.
- [41] C. T. Group. ETH Zurich Department of Information Technology and Electrical Engineering. [Online]. Available: <http://www.nari.ee.ethz.ch/commth/research/>
- [42] K. Lee, J. Ho, and D. Kriegman, "Acquiring linear subspaces for face recognition under variable lighting," *IEEE Trans. Pattern Anal. Mach. Intelligence*, vol. 27, no. 5, pp. 684–698, 2005.
- [43] S. A. Nene, S. K. Nayar, and H. Murase, "Columbia object image library (COIL-20)," Columbia University, Tech. Rep., 1996.
- [44] —, "Columbia object image library (COIL-100)," Columbia University, Tech. Rep., 1996.
- [45] D. Cai, X. He, J. Han, and T. S. Huang, "Graph regularized non-negative matrix factorization for data representation," *IEEE Transactions on Pattern Analysis and Machine Intelligence*, vol. 33, no. 8, pp. 1548–1560, 2011.
- [46] J. Bruna and S. Mallat, "Invariant scattering convolution networks," *IEEE transactions on pattern analysis and machine intelligence*, vol. 35, no. 8, pp. 1872–1886, 2013.